

Article

Heat Transfer Analysis of Methane Hydrate Sediment Dissociation in a Closed Reactor by a Thermal Method

Jiafei Zhao, Chuanxiao Cheng *, Yongchen Song *, Weiguo Liu, Yu Liu, Kaihua Xue, Zihao Zhu, Zhi Yang, Dayong Wang and Mingjun Yang

Key Laboratory of Ocean Energy Utilization and Energy Conservation of Ministry of Education, Dalian University of Technology, Dalian 116023, China; E-Mails: jfzhao@dlut.edu.cn (J.Z.); liuwg@dlut.edu.cn (W.L.); liuyu@dlut.edu.cn (Y.L.); xuekh@163.com (K.X.); zhuzihao.dlut@gmail.com (Z.Z.); yangzhi.dlut@gmail.com (Z.Y.); wangdy@dlut.edu.cn (D.W.); yangmj@dlut.edu.cn (M.Y.)

* Authors to whom correspondence should be addressed; E-Mails: ccxring@gmail.com (C.C.); songyc@dlut.edu.cn (Y.S.); Tel.: +86-411-84706608; Fax: +86-411-84708015.

Received: 15 March 2012; in revised form: 13 April 2012 / Accepted: 18 April 2012 /

Published: 2 May 2012

Abstract: The heat transfer analysis of hydrate-bearing sediment involved phase changes is one of the key requirements of gas hydrate exploitation techniques. In this paper, experiments were conducted to examine the heat transfer performance during hydrate formation and dissociation by a thermal method using a 5L volume reactor. This study simulated porous media by using glass beads of uniform size. Sixteen platinum resistance thermometers were placed in different position in the reactor to monitor the temperature differences of the hydrate in porous media. The influence of production temperature on the production time was also investigated. Experimental results show that there is a delay when hydrate decomposed in the radial direction and there are three stages in the dissociation period which is influenced by the rate of hydrate dissociation and the heat flow of the reactor. A significant temperature difference along the radial direction of the reactor was obtained when the hydrate dissociates and this phenomenon could be enhanced by raising the production temperature. In addition, hydrate dissociates homogeneously and the temperature difference is much smaller than the other conditions when the production temperature is around the 10 °C. With the increase of the production temperature, the maximum of ΔT_{oi} grows until the temperature reaches 40 °C. The period of ΔT_{oi} have a close relation with the total time of hydrate dissociation. Especially, the period of ΔT_{oi} with production temperature of 10 °C is twice as much as that at other temperatures. Under

these experimental conditions, the heat is mainly transferred by conduction from the dissociated zone to the dissociating zone and the production temperature has little effect on the convection of the water in the porous media.

Keywords: methane hydrate; thermal method; dissociation; temperature difference; heat transfer

1. Introduction

Gas hydrates are known to occur worldwide in locations such as the permafrost regions as well as beneath the sea [1,2]. They have an important impact on flow assurance; safety issues; energy recovery; transportation and climate change [3,4]. It has been estimated that the World resources of carbon trapped in hydrates is twice the amount of carbon in known fossil fuel deposits [5,6]. Due to this potential resource, the problems associated with production of natural gas hydrate have become of greater interest to the more and more countries [7,8]. Heat transfer, as one of the three main mechanisms of hydrate production, has an increasingly significant influence on hydrate safety and efficient exploitation [9]. One of the key requirements of any production technique is to provide the heat necessary for the endothermic reaction of hydrate decomposition, which is determined by heat transfer [10], so the heat transfer analysis of hydrate-bearing sediments is a controlling factor for all production techniques.

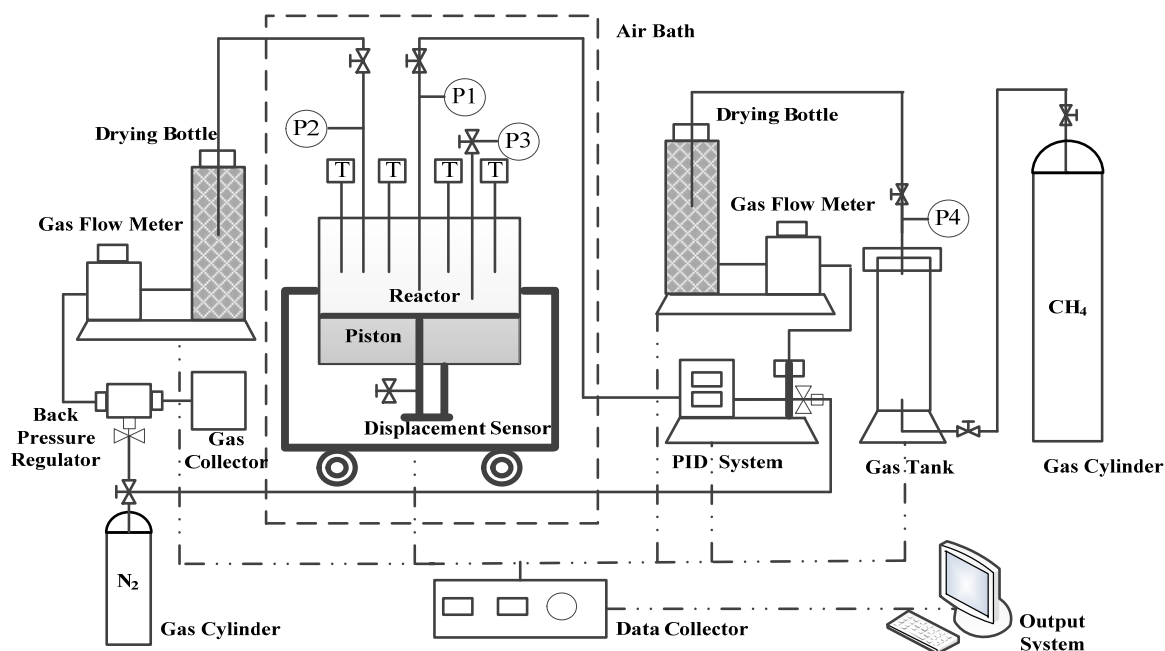
In recent years, a variety of experimental and theoretical works focused on heat transfer involved in dissociation of gas hydrates have been reported. Kamath *et al.* [11] reported the first instance of measurements and made the nucleate boiling correlations of heat transfer under gas-solid liquid equilibrium conditions. They calculated the heat transfer coefficients and the rates of dissociation and proved that the rate of heat transfer is a power function of the temperature driving force, ΔT , which is the difference between the temperature of the warm fluid used to dissociate the hydrate and the temperature of the dissociating hydrate. Their results also showed that the dissociation process is limited by heat transfer and the heat transfer rate depends on the rate of circulation of the warm fluid used to dissociate the hydrate. Selim *et al.* [12,13] viewed heat transfer during hydrate dissociation as a moving-boundary ablation process and showed that their model fits hydrate dissociation data to within 10%. However, the results of these studies are only useful in modeling pure hydrate dissociation processes. Furthermore, they also presented a physical model that describes hydrate dissociation in porous media under thermal stimulation [7]. This model also considered heat transfer during hydrate dissociation as a moving-boundary and the latter separates the dissociated zone, which contains gas and water, from the un-dissociated zone, which contains the hydrate. The results proved that energy efficiency ratio is independent of time, and depends only on the parameters of the system and the boundary and initial conditions. Pooladi-Darvish *et al.* [10] presented a system model to study the effects of conductive and convection heat flow on gas production from natural hydrates by depressurization. The results depicted that thermal conductivity of sediments has a significant effect on the heat transfer of hydrate decomposition and a raise of the convection of hydrate sediment may lead to the decrease of heat capacity of the whole hydrate sediment which would slow down the production

rate. Iida *et al.* [14] observed tetrahydrofuran hydrate formation and growth, or melting in a macroscopically one-dimensional heat-transfer system under atmospheric pressure. They analyzed the heat transfer from, or to the hydrate-solution interface across the hydrate and solution layers. Their results indicated that the interface became increasingly wavy with the thickening of the solution layer which is induced by free convection in the solution layer when the boundary temperature increased and the experimental run exhibited an inflection point that corresponds to the inception of the free-convection-dominated heat transfer in the growing liquid-solution layer. The experimental data are also in general agreement with that predicted by theoretical analyses of transient conductive and/or free-convective heat transfer from/to the hydrate-solution interface. A series of experimental studies were conducted on visual observation of the pore-scale dissociation of hydrate crystals caused by a temperature increase in a closed system and the mechanism of the dissociation of the methane hydrate crystals was discussed considering the heat and mass transfer of methane around the dissociating methane hydrate crystals. Their results demonstrate that the methane molecules released from these hydrate crystals were transferred through the liquid water phase to the methane gas slugs surrounding these hydrate crystals [15–17]. A new re-gasification system, in which warm water penetrates through a bed of gas hydrate pellets for the recovery of gas from stored hydrate, was investigated to achieve a more compact and more efficient re-gasification system by Tanaka *et al.* [18,19]. The heat transfer in quiescent hydrate formation/dissociation reactor has been studied by Bei Liu *et al.* [20,21]. Their results indicated that a stage of buffered dissociation occurred when the hydrates was heated to temperatures approaching the melting point of ice. During this period, the sample temperature remains within a narrow range near the ice point, rises slowly as the hydrate dissociation proceeds, and the corresponding dissociation rate is very low. The buffering effect can be eliminated and the dissociation rate can be improved by increasing the temperature of the heating water or reducing the dissociation pressure. Zhang *et al.* [22] also did research on thermally induced evolution of phase transformations. Numerical simulation shows that the temperature is continuous and the temperature gradient is discontinuous at the phase transformation front.

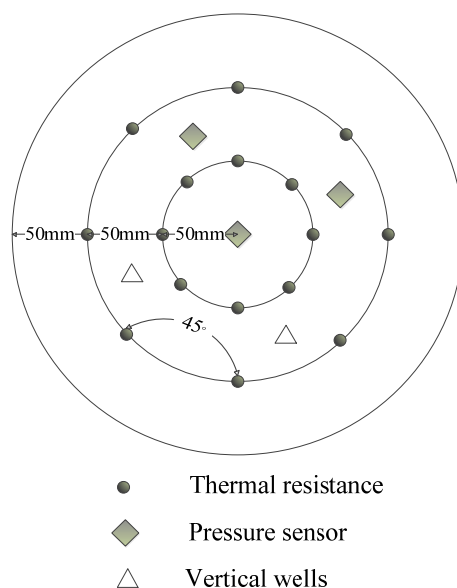
Up to now, relatively little attention has been given to the problem because of the inherent complexity encountered when dealing with porous media coupled with phase transformation and motion of the interface [10,23]. Due to the limited amount of experimental work on heat transfer during hydrate dissociation in porous media, the various effects are not fully understood and a number of critical issues remain unresolved. The heat transfer of hydrate dissociation in porous media in a closed reactor by a thermal method has not been systematically studied. In this paper, a 5 L volume reactor was used to investigate the heat transfer characteristics of hydrates in porous media during the dissociation process in a closed reactor by a thermal method. Sixteen thermal resistance thermometers were distributed uniformly in two circles in the reactor. The hydrate decomposes at a different production temperature in a closed reactor. The relation of temperature difference of the different positions in the radial direction and the hydrate dissociation rates were obtained. The characteristics of methane hydrate decomposition characteristic were also investigated.

2. Apparatus and Materials

A schematic diagram of the experimental device is illustrated in Figure 1. The primary components of the apparatus are a stainless steel reactor, an air bath system, and a data collection system.

Figure 1. Schematic diagram of the experimental apparatus.

The reactor is 300 mm in internal diameter, 70 mm in inside height and has a volume of 5 L. It is made of stainless steel which can sustain pressures up to 20 MP. There is a movable piston in the reactor which is used to press the porous media and change the volume of the reactor. The effective volume of reactor could be obtained by using the displacement sensor which is attached on the piston. A gas flow meter is used to obtain the amount of gas injected. The PID system could control the gas steadily injected into the reactor under the same pressure difference which is useful to make the gas flow meter more accurate. N_2 pressure is used to provide the power for the PID system and back pressure regulator. Uniform quartz glass beads (AS-ONE, Co., Ltd., Osaka, Japan) BZ-04 (0.350–0.500 mm, average 0.4 mm) were used to simulate the porous media. The porosity of the porous media is 36.1%. The reactor is enclosed in an air bath which can maintain at a constant temperature ranging from 253 to 323 K with a precision of ± 0.1 K. The upper and bottom ends of the reactor were capped with thermal insulation foam and the heat mainly flows into the reactor through the walls of the cylinder. The temperature and pressure profiles are measured by 16 Pt. 1000 thermal resistance thermometers and three pressure sensors which have a precision of ± 0.1 K and ± 0.1 MP, respectively, placed on top of the reactor in different positions. The details of the position of the thermal resistance thermometers and pressure sensors are shown in Figure 2. All the data was detected and recorded every 30 s.

Figure 2. The distribution of thermal resistance thermometers and pressure sensors.

3. Procedure

3.1. Hydrate Formation

First, the reactor was cleaned with deionized water. Then dry BZ-04 quartz sand was tightly packed in the reactor and saturated with deionized water and the amounts of both were recorded. Then the reactor was closed and the piston used to press the porous media until the axial pressure comes to 10 MP. After that, the axial pressure was decreased to zero and the reactor was evacuated for 10 min to remove air using a vacuum pump. Then the methane was dried and charged into the reactor steadily until the pressure rose to the given pressure of 8.4 MP at 20.5 °C and the flow meter and PID system are used to measure and record the amount of methane gas during this process. Finally, the air bath system was turned on and the temperature kept at 1 °C which is higher than the ice point to avoid the formation of ice in order to remove the buffer effect which is observed by Pang *et al.* [14,15]. The main materials used in the experiment are listed at Table 1. When the pressure drop in the system is less than 0.1 MP over 3 h, the hydrate formation process is assumed to be complete.

Table 1. Experimental materials.

Sample	Specification	Supply
CH ₄	99.999%	Dalian DATE special gas
Deionized water	Pure	Laboratory
Quartz sand	BZ-04, Φ -0.361, ρ -2.18 g/cm ³	AS-ONE corporation (Japan)

3.2. Hydrate Dissociation

After hydrate samples were formed completely as described above, it came to the hydrate dissociation stage. The reactor was kept closed and the air bath was set at a different temperature, which simulates the hydrate production during the preservation stage and hydrate dissociation under thermal stimulation in porous media [24]. Seven groups of hydrate decomposition experiments under

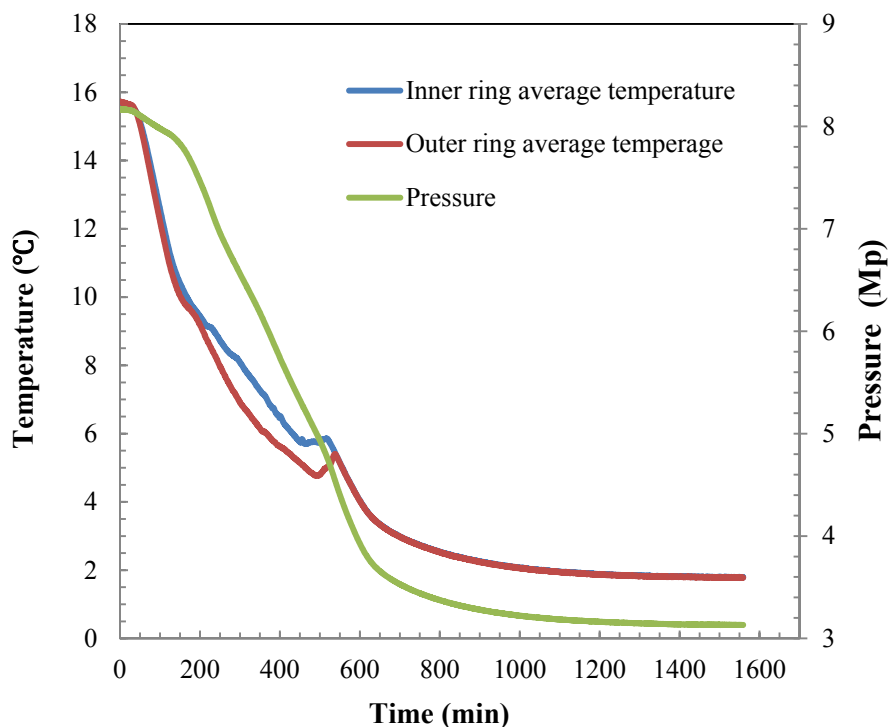
different temperatures were presented in this paper. The temperature of the air bath was separately set at 10, 15, 20, 25, 30, 35 and 40 °C for the hydrate dissociation. The process of hydrate decomposition was described by the pressure decrease and temperature difference. As the reactor was closed, the pressure increased during the dissociation stage. When the pressure remains steady for 2 h, it means the end of the dissociation. After the hydrate dissociation, the temperature of air bath was set at 1 °C for the next group of experiment so we could maintain the same hydrate sediment sample in each group.

4. Results and Discussion

4.1. Hydrate Formation Characteristics in the 5 L Reactor

Figure 3 shows the hydrate formation process. With the decrease of temperature, the hydrate begins to form at around of 11 °C, which is below the equilibrium condition (about 11.5 °C) and the pressure decreases sharply. As the each eight thermal resistance thermometers were placed in the same radial position and the eight inner ring or outer ring thermal resistance thermometers show similar values, the average temperature of the eight thermal resistance thermometers could represent the temperature of hydrate at same the radial position.

Figure 3. The pressure and temperature curve during the hydrate formation.

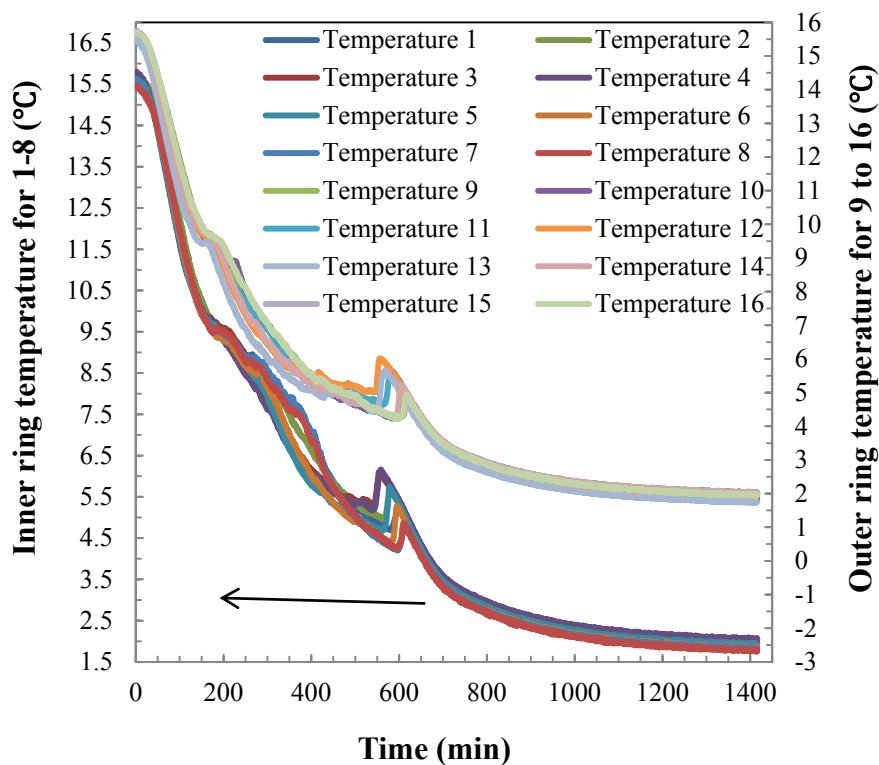


In addition, the detailed values measured by each thermal resistance thermometer were also presented in Figure 4. All the formation experiments show the same results, which indicates that the hydrate sediment sample in each group is similar. As shown in Figure 3, before the hydrate formation, the temperatures in different positions of the reactor are in accordance and decreased sharply. There is no phase change phenomenon in this process. The heat of the hydrate sediment flows out mainly by conduction. When the temperature reaches the equilibrium condition and hydrate begins to form, there

is an apparent temperature difference between the two radial positions. All seven groups show the same phenomenon in the hydrate formation stage. The temperature difference increases at first and then disappears when the hydrate formation is finished.

There are two main reasons for this phenomenon. First, the hydrate formation is exothermic process and the heat around outer ring position could be removed easily due to the temperature difference between the steel wall and the outer ring position. While, the heat around the inner ring position could not remove out quickly as the low thermal conductivity of porous media around, which could lead to the high temperature difference. Second, the thermal properties of hydrate sediments would be changed as the component of the hydrate sediment changed and the hydrate formation has an effect to the heat transfer properties.

Figure 4. The temperature curves of the 16 thermal resistance thermometers during hydrate formation.



At the later stage of hydrate formation, there is a significant temperature increase with a sharp pressure decrease, which indicates a large amount of hydrate formation at the positions of the thermal resistance thermometers. As the thermal resistance thermometers were placed in the middle porous media, the hydrate formation at the upper surface could not be detected immediately and there is no significant temperature raise, but the temperature decrease rate became smaller than the conditions that have no hydrate formation, which indicated that a large amount of hydrate was formed and heat released. This is the main reason why the sharp temperature increase and temperature peak which are used to estimate the formation of hydrate did not appear. Therefore, there are two stages for the large amount of hydrate formation. The hydrate at the upper surface of the reactor forms at first, with the gas penetrating into the porous media, the hydrate then begins to form in the middle of the reactor. The

phenomenon has been proven by other researchers [14,22]. As shown in Figure 4, the detailed temperature curves of the 16 thermal resistance thermometers have the same trend and the small differences of each thermal resistance thermometers indicated that the hydrate in different position formed non-simultaneously. In addition, the similar temperature during hydrate formation also indicated that the amount of hydrate formed in different positions is uniform.

In this study, the gas production mass with pressure increase was calculated. The saturation of hydrate was measured by a weighing method under extremely low temperatures. When all seven groups of experiments were finished, the hydrate formed again. After the hydrate formation, the temperature of air was set at $-5\text{ }^{\circ}\text{C}$ which would keep the hydrate stable when we opened the reactor. Then the hydrate sediment was taken out and weighed at low temperature. The change of the sediment's weight is the weight of gas in the hydrate. The saturation is calculated as follows:

$$S_H = V_H/V_0$$

$$V_H = n_g \times M_{(\text{CH}_4 \cdot 5.75\text{H}_2\text{O})}/\rho_H, \quad n_g = m_g/M_g, \quad V_0 = (m_s/\rho_s) \times \Phi_0$$

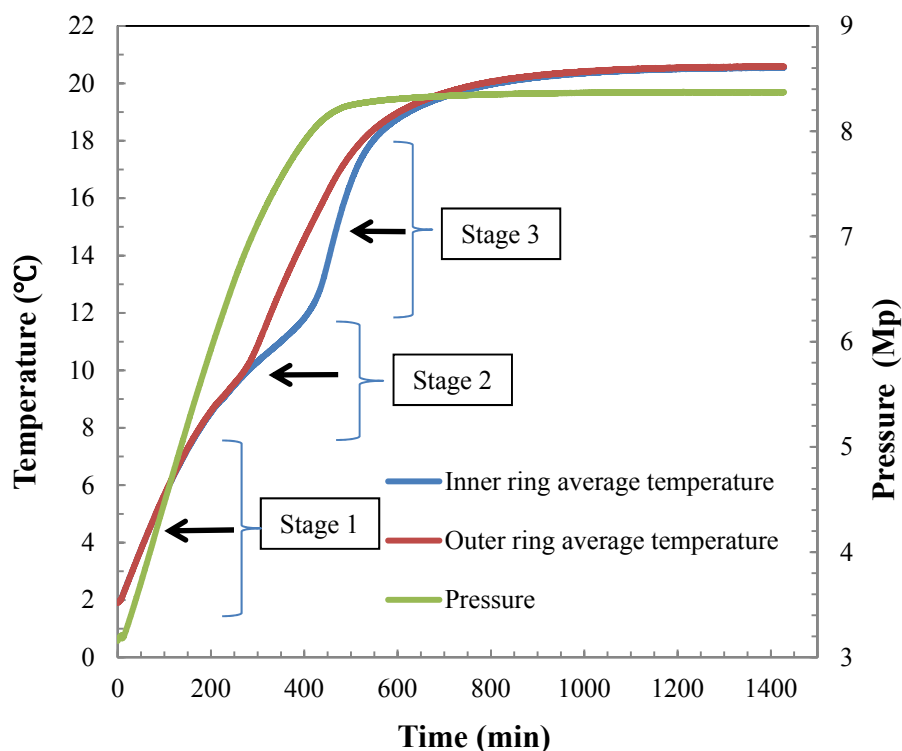
where S_H —saturation, V_0 —voids volume of porous media, m_s —mass of BZ-04, ρ_s —density of BZ-04, 2.6 g/cm^3 ; $\rho_H = 0.918\text{ g/cm}^3$; Φ_0 —porosity of BZ-04, 0.316. The overall saturation of hydrate in this study is about 64.78%. This study assumes that the saturation of the seven group is similar, which indicates that the sample of the hydrate sediment has no effect on the dissociation. In addition, this study also examined the saturation by calculating the amount of methane consumed during hydrate formation and the results showed a similar value.

4.2. Hydrate Dissociation Process

Figure 5 shows the pressure and temperature curves during hydrate dissociation under $25\text{ }^{\circ}\text{C}$. After setting the temperature of air bath to $25\text{ }^{\circ}\text{C}$ (or another temperature), the temperature of the air bath increased at a rate of $2.1\text{ }^{\circ}\text{C}/\text{min}$ and the temperature would soon reach the set value. As the stainless steel wall thermal resistance is small, the heat quickly flows into the surface of the hydrate sediments. Then, hydrates have not dissociated, so the pressure just increases with the temperature slowly (0–20 min). There is no temperature difference in the hydrate sediments. However, this period is too short to be observed in Figure 5. The experiments conducted show that the temperature at the inner ring position (T_i) and the temperature at outer ring position (T_o) are in agreement before and after the hydrate dissociation, while there is a significant temperature difference (ΔT_{oi}) during the hydrate dissociation process. The ΔT_{oi} changed with the different wall temperature which is discussed in the following section.

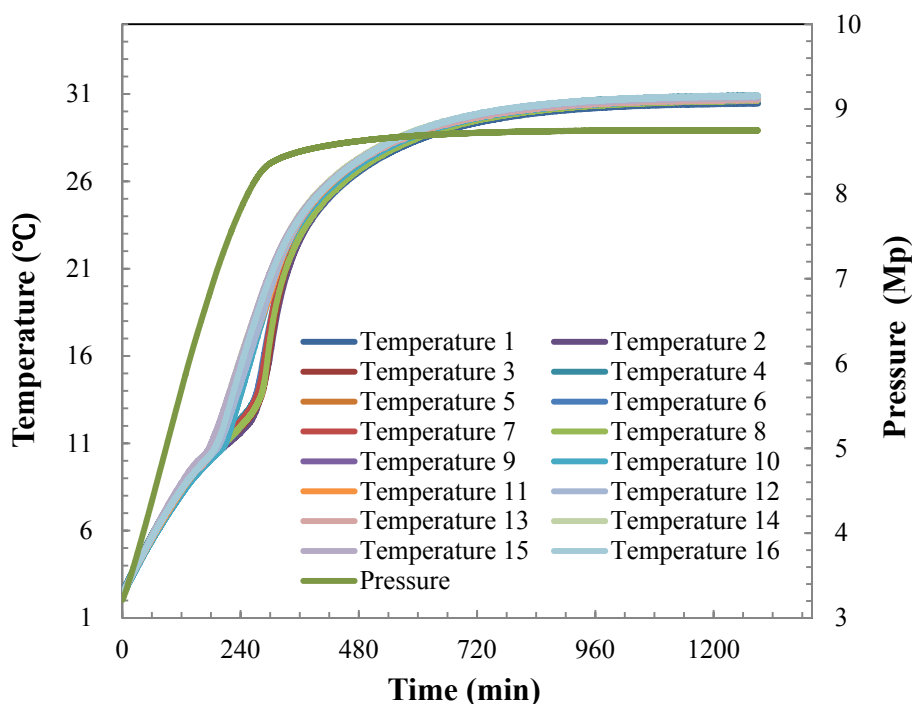
As shown in Figure 5, for the two temperature curves, a similar trend of change appeared during the hydrate dissociation in different radial directions. There is a delay between the two temperature curves. The hydrate in the outer ring position dissociated first and then the hydrate in the inner ring position decomposed. This also proven the existence of a hydrate dissociation interface and moving boundary which has been observed by Selim *et al.* [12,13]. For the temperature, there are three stages during the hydrate dissociation. In stage 1, the hydrate around the steel wall surface begins to decompose and the pressure increases sharply, which also proves that a large amount of hydrate was dissociated. In addition, the accordance of temperature at inner ring position and outer ring position indicated that to hydrate dissociation occurred there.

Figure 5. The pressure and temperature curve during the hydrate decomposition at 20 °C.



In the early part of stage 1, there is a slight inflection in the temperature curves. As the hydrate in the outer ring position started to decompose, the rate of increase of T_o becomes slightly slow, as shown in Figure 5. This phenomenon is mainly caused by the heat absorbed by the hydrate dissociated around the thermal resistance thermometers at the outer ring position. Furthermore, the gas produced during the dissociation could decrease the thermal conductivity of the hydrate sediments and the thermal capacity. Pooladi-Darvish [10] also proved that the increase of convection caused by produced gas may lead to a decrease of heat capacity and the gas production rate.

At the middle of stage 2, the temperature increase rate grows sharply and the temperature rises linearly which indicates the hydrate at outer ring position has dissociated completely. Then the temperature of the internal sediments is above the equilibrium temperature and the hydrate at inner ring position begins to decompose. In addition, the ΔT_{oi} increases at first and then disappears gradually. That because hydrate at inner ring position decomposes and absorbs the heat from the surrounding sediment, mainly from dissociated zone at the outer ring position and when the heat flow could not meet the heat needs for hydrate dissociation, the ΔT_{oi} term appears. The ΔT_{oi} increases with the hydrate dissociation rate and disappears until the end of the dissociation. Therefore, the ΔT_{oi} reflects the degree of the hydrate dissociation. When it comes to stage 3, the pressure increase stops and the ΔT_{oi} disappears, which indicates the end of the dissociation in the reactor. It is the dissociation of hydrate and the heat flow at inner ring that mainly cause the temperature difference. Therefore, during the three stages, the change of ΔT_{oi} also proves that heat transfer during hydrate dissociation is a moving-boundary ablation process. Moreover, the detailed temperature curves of the 16 thermal resistance thermometers during the hydrate decomposition at 30 °C are also presented in Figure 6. The small differences of each thermal resistance thermometer indicate that the hydrate in different positions dissociated uniformly.

Figure 6. The pressure and temperature curve during the hydrate decomposition at 30 °C.

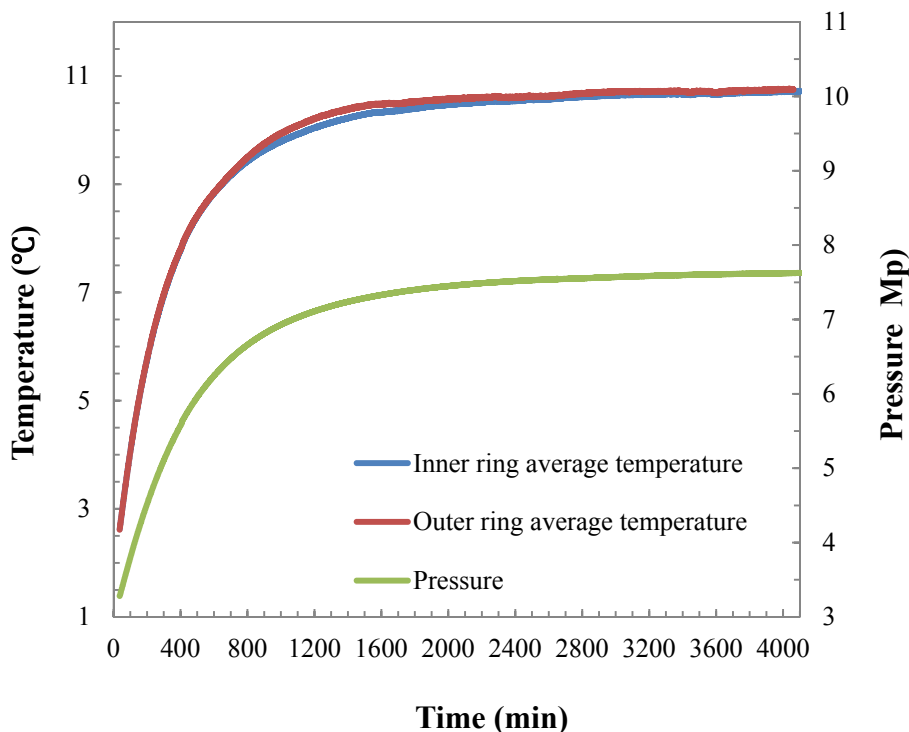
In the Messoyakha field production stage (IV), the well was closed and came to the preservation phase. As the temperature and pressure are above the equilibrium conditions, therefore the hydrate continues to dissociate and pressure increases [25–27]. This study stimulates the hydrate dissociation in the preservation stage. The environmental temperature was set as 10 °C, which is similar to the Messoyakha field. As shown in Figure 7, there is no significant temperature difference between the inner and outer parts of the reaction, which indicates that the hydrate dissociates uniformly in different positions of the reactor. As the pressure and temperature are near the equilibrium conditions, the hydrate dissociates slowly than the other groups, about three times as much as that at other temperatures. Since the hydrate decomposes slowly, the heat needed can be compensated by the heat flow from the air bath which results in the uniform dissociation of hydrate. In addition, the thermal properties of hydrate sediments change slowly, which has little impact on the heat flow of the reactor. This is meaningful in controlling the safety of the geology in hydrate exploitation.

4.3. Heat Transfer Analysis during Hydrate Dissociation

At the dissociation stage, the temperature of the air bath comes to the set values in a few minutes. The heat flows into reactor through the stainless steel wall. As the thermal conductivity of stainless steel wall is 16 W/mK, which is much larger than that of the hydrate sediment, the temperature of the inner and outer ring walls of the reactor is assumed to be same. Before the temperature of the wall increases to the phase equilibrium condition, the hydrate has not dissociated and there is no phase change in the reactor. The heat conduction is the controlling heat transport process while this happens. The accordant and homogenous temperatures in different positions of the reactor also proved that. With the temperature of the wall rising, the hydrate near the wall begins to decompose. The dissociation of solid hydrate in porous media to liquid water and gas is a phase change process which involves three phases. This process in the presence of sand is an unsteady process. This unsteady state

is expected since as the hydrate dissociates, the sand present in the unconsolidated hydrate sediments starts building a layer in front of the un-dissociated hydrate zone.

Figure 7. The pressure and temperature curve during the hydrate decomposition at 10 °C.



Even if the temperature of the wall of the reactor and the temperature of the hydrates are held constant, the increase in the resistance to heat transfer due to the sand layer reduces the interfacial heat transfer and the rate of dissociation. In order to analyze the data obtained for unsteady state dissociation of methane hydrate in porous media, the following assumptions were made in this study: The presence of sand does not affect the equilibrium dissociation pressure for pure methane hydrates and the uniform glass bead is considered to be an isotropic porous medium. There are three different zones in the reactor during the dissociation process: dissociated zone, dissociating zone, hydrate zone. The dissociated zone is composed of uniform glass beads and water. In order to analyse the free convection of water in the dissociated zone, the Rayleigh number is calculated as follows [28]:

$$R_{\alpha} = \frac{Kg\beta(T_w - T_{\infty})H}{\vartheta\alpha_e}$$

where:

$$\alpha_e = \frac{\lambda_e}{(\rho c)_e}$$

$$\lambda_e = \lambda_s(1 - \varepsilon) + \varepsilon\lambda_w$$

$$(\rho c)_e = (\rho c)_s(1 - \varepsilon) + (\rho c)_w$$

R_{α} = Rayleigh number

H = Characteristic length (in this case, the height of hydrate porous media)

g = acceleration due to gravity

T_w = Surface temperature (temperature of the wall of reactor)

T_∞ = Quiescent temperature (temperature in the dissociated zone)

ν = Kinematic viscosity of water

α_e = Effective thermal diffusivity

β = Thermal expansion coefficient

λ_e = Effective thermal conductivity

λ_s = Thermal conductivity of sand

λ_w = Thermal conductivity of water

ε = Porosity of glass beads

ρ = Density (kg/m^3)

c = Specific heat capacity ($\text{J}/(\text{kg}\cdot\text{K})$)

In the above, the water properties ν , α , and β are evaluated at the film temperature, which is defined as: $T_f = (T_w - T_\infty)/2$. According to the calculated results, $R_a = G_r P_r \ll 10^3$, the natural convection of water caused by temperature difference has little effect on the heat transfer in this zone, so the convection could be ignored and the heat is mainly transferred by conduction. The hydrate zone still has no phase change and the heat conduction is still dominated by heat-transfer. While in the dissociating zone, the hydrate decomposes into water and methane and heat of hydrate dissociation is absorbed. With the accumulation of dissociated methane, the local pressure in the porous media increases and then the dissociated methane permeates the hydrate zone into the upper part of the reactor under the pressure gradient. The methane produced which rises through the porous media could increase the heat transfer to the interface from the dissociated zone. There have been some visual researches on the hydrate dissociation process which have observed the mass transfer of produced methane [17], which is useful to analyze the heat transfer during hydrate dissociation. Kamath [23] also calculated the heat flux from the water to the sand zone and developed an unsteady state model for heat transfer in a manner similar to the Rohsenow nucleate boiling correlation. However, it is still difficult to characterize the heat transfer phenomena associated with dissociation of hydrates in sediments exactly. The combination of *in situ* observation and high-precision temperature sensor could be an effective method. In the experiments, it is assumed that the heat is transferred only by conduction from the dissociated zone to the dissociating zone and the temperature profile in the sand zone is uniform. The heat flux from the walls of the reactor to the dissociated zone is equated to the heat flux from the sand to the hydrates. The increase of dissociation rate could decrease the temperature of the dissociated zone which could increase the heat flux to compensate the temperature from the dissociated zone to the wall. With the drop of dissociation rate, the heat flux decreases. Despite the great suppression on the convection of glass beads, the effect of gas permeate on the heat transfer is still unclear. In addition, the residual methane in the porous media which has been observed after the hydrate dissociation would decrease the effective thermal conductivity and heat capacity of porous media and this phenomenon has also been proven by Pooladi-Darvish [10].

4.4. Temperature Difference during the Hydrate Dissociation

In this study, the hydrate dissociates in a closed reactor by thermal method. If the hydrate in local place decomposes too quickly that the heat from the air bath could not compensate, there will be a

temperature difference in the radial direction. That means there are large amount hydrate dissociation and the change of thermal properties of hydrate. The temperature difference in the hydrate sediment is the main driving force for the dissociation. Figures 8 and 9 show the ΔT_{oi} with different production environment temperatures.

Figure 8. ΔT_{oi} with different environmental temperatures.

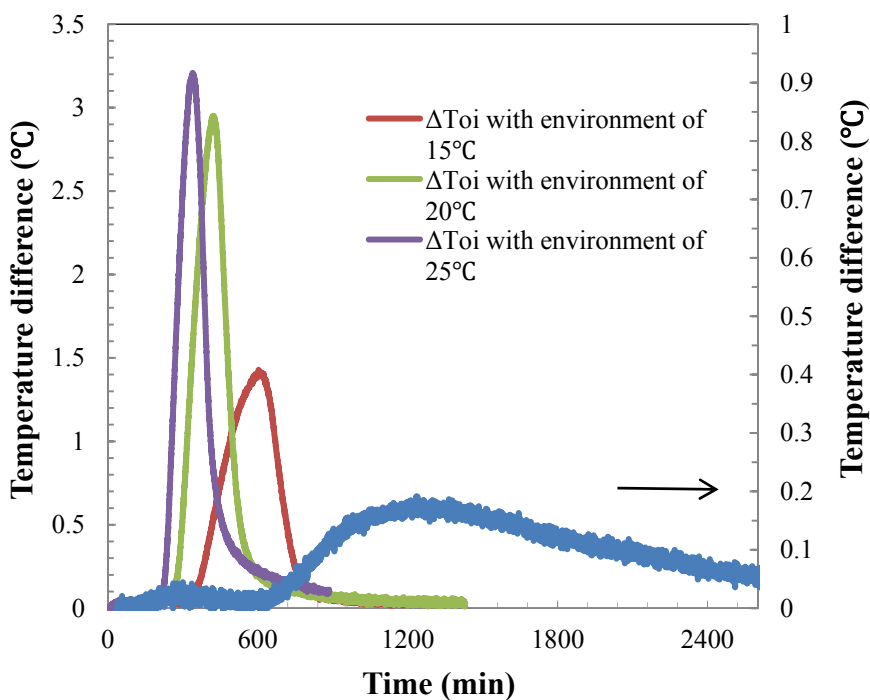
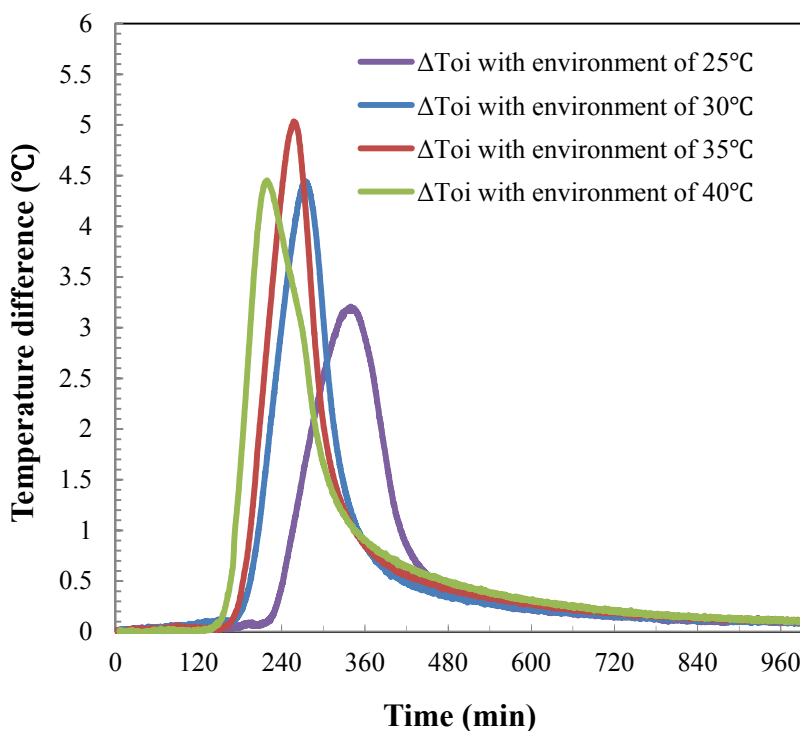


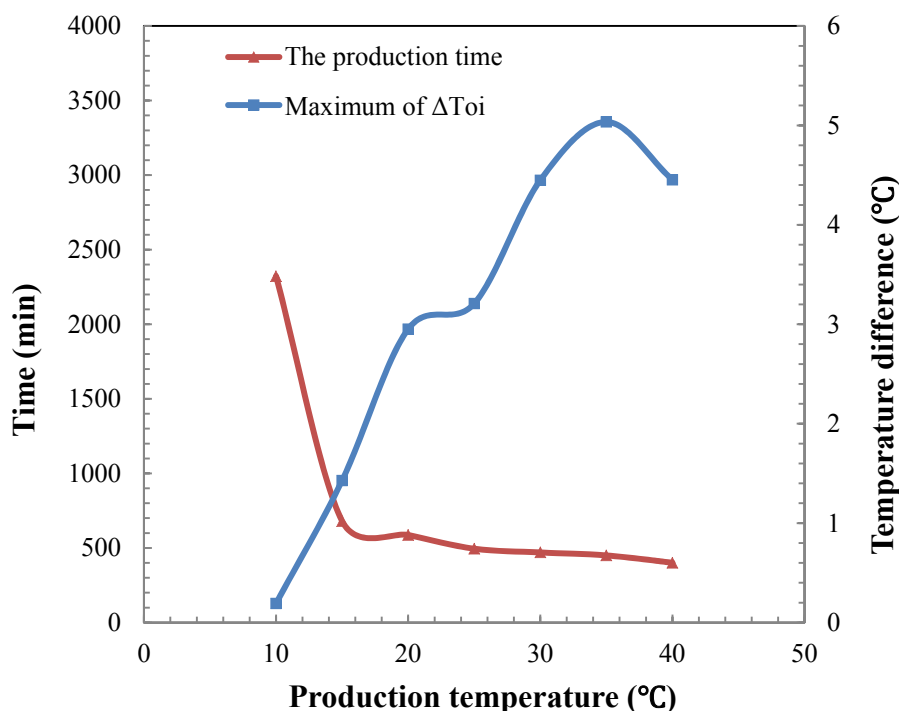
Figure 9. ΔT_{oi} with different environmental temperatures.



The results indicate that with the increase of the environmental temperature (air bath temperature), the maximum ΔT_{oi} grows except for the 40 °C group. This result also proves that the ΔT_{oi} is caused both by the dissociation rate and the production temperature. With the disappearance of the temperature difference, the process of hydrate dissociation is finished. Therefore, the period of the ΔT_{oi} determines the total duration of the hydrate dissociation. When the production environmental temperature is at about 10 °C, the period of ΔT_{oi} is twice as long than for other groups.

The total production times and maximum of ΔT_{oi} with different production environment temperatures are shown in Figure 10. The production time generally decreases with the temperature of the air bath. In addition, the production time at different production temperatures are similar, except at 10 °C. The changes of temperature difference indicate that the heat transfer is affected by the thermal properties of the hydrate sediments. When the temperature and pressure conditions are higher than the equilibrium condition, the hydrate around the wall decomposes first and absorbs heat. Then the remaining heat flows into the inner ring of the reactor, which leads to the temperature difference phenomenon.

Figure 10. Maximum of ΔT_{oi} and production time with different production temperature.



However, at around the equilibrium conditions, the hydrate dissociates slowly and homogeneously and the temperature difference is much smaller than under the other conditions. Kamath *et al.* [23] also proved the dissociation of hydrates in sand is an unsteady state process, because as hydrate dissociates, the sand starts building a layer on the top of the core increasing the resistance to heat transfer. It was also considered that the heat transfer from the dissociated zone to the dissociating zone takes place by conduction through the sand zone. When the production temperature increases, the dissociation rate and the heat absorbed for dissociation grows. The heat conducted from the dissociated zone could not supply this. Therefore, the temperature difference could be increased by increase the production temperature. However, when the production temperature increases to 40 °C, the ΔT_{oi} is little smaller

than that of 35 °C. That may be determined by saturation of the hydrate which has the effect of absorbing heat from the surroundings.

5. Conclusions

In this paper, experiments were conducted to examine the heat transfer performance during hydrate formation and dissociation using a 5 L volume reactor. The hydrate was dissociated in a closed reactor by the thermal method. From the experimental results, the following conclusions can be drawn:

(1) An apparent temperature difference is obtained between the two radial positions in the reactor when the hydrate begins to form, which is led by the exothermic process and the change of the thermal properties of hydrates. There are two stages for the formation of large amounts of hydrate. The hydrate at the surface of the reactor forms at first, with the decreasing of temperature and gas penetrating into the porous media, the hydrate then begins to form in the middle of the reactor.

(2) There are three stages in the hydrate dissociates process in a closed reactor by the thermal method, which is caused by the rate of dissociation and heat flow. The delay of hydrate dissociation between the inner ring and outer ring positions indicated the existence of a dissociation interface and moving boundary. An apparent temperature difference appears in the hydrate sediment during the dissociation process. However, the hydrate dissociates homogeneously and the temperature difference is much lower than under other condition when the production environment temperature is around 10 °C. Under this experimental conditions, the temperature of the convection of water in porous media is ignored. The heat is mainly conducted into the dissociated zone and into the dissociating zone.

(3) With the increasing temperature of the air bath, the maximum of ΔT_{oi} grows except when the temperature comes to 40 °C. The period of ΔT_{oi} are in accordance with the total time of hydrate dissociation. The period of ΔT_{oi} with environment of 10 °C is about twice as long than in the other groups.

Acknowledgments

This study is supported by the National High Technology Research and Development Program of China (863 Program, Grant No. 2006AA09A209), the National Science and Technology Major Project, China (Grant No. 2011ZX05026-004), the Natural Science Foundation of China (Grant No. 51006017), and Major State Basic Research Development Program of China (973 Program, Grant No. 2009CB219507).

References

1. Kerkar, P.; Jones, K.W.; Kleinberg, R.; Lindquist, W.B.; Tomov, S.; Feng, H.; Mahajan, D. Direct observations of three dimensional growth of hydrates hosted in porous media. *Appl. Phys. Lett.* **2009**, *95*, 024102:1–024102:3.
2. Sloan, E.D. *Clathrate Hydrates of Natural Gas*, 2nd ed.; Marcel Dekker Inc: New York, NY, USA, 1998.
3. Sloan, E.D. Fundamental principles and applications of natural gas hydrates. *Nature* **2003**, *426*, 353–363.

4. Zhao, J.; Yao, L.; Song, Y.; Xue, K.; Cheng, C.; Liu, Y.; Zhang, Y. *In situ* observations by magnetic resonance imaging for formation and dissociation of tetrahydrofuran hydrate in porous media. *Magn. Reson. Imaging* **2011**, *29*, 281–288.
5. Chen, G.J.; Sun, C.Y.; Ma, Q.L. *Science and Technology of Gas Hydrate (in Chinese)*; Chemical Industry Press: Beijing, China, 2007; pp. 3–10.
6. Gabitto, J.F.; Tsouris, C. Physical properties of gas hydrates: A review. *J. Thermodyn.* **2010**, *2010*, 1–12.
7. Selim, M.S.; Sloan, E.D. Heat and mass transfer during the dissociation of hydrates in porous media. *AIChE J.* **1989**, *35*, 1049–1052.
8. Fan, S.S. *Storage and Transport Technology of Natural Gas Hydrate (in Chinese)*; Chemical Industry Press: Beijing, China, 2005; pp. 2–10.
9. Hong, H.; Pooladi-Darvish, M.; Bishnoi, P.R. Analytical modeling of gas production from hydrates in porous media. *J. Canadian Petrol. Technol.* **2003**, *42*, 45–56.
10. Pooladi-Darvish, M.; Hong, H. *Effect of Conductive and Convective Heat Flow on Gas Production from Natural Hydrates by Depressurization, Advances in the Study of Gas Hydrates*; Taylor, C., Kwan, J., Eds.; Springer: New York, NY, USA, 2004; pp. 43–65.
11. Kamath, V.A.; Holder, G.D.; Angert, P.F. Three phase interfacial heat transfer during the dissociation of propane hydrates. *Chem. Eng. Sci.* **1984**, *39*, 1435–1442.
12. Selim, M.S.; Sloan, E.D. Modeling of the Dissociation of an *In situ* Hydrate. In *SPE California Regional Meeting*, Bakersfield, California, CA, USA, 27–29 March 1985; p. 13597.
13. Ullerich, J.W.; Selim, M.S.; Sloan, E.D. Theory and measurement of hydrate dissociation. *AIChE J.* **1987**, *33*, 747–752.
14. Iida, M.; Mori, H.; Mochizuki, T.; Mori, Y.H. Formation and dissociation of clathrate hydrate in stoichiometric tetrahydrofuran—water mixture subjected to one-dimensional cooling or heating. *Chem. Eng. Sci.* **2001**, *56*, 4747–4758.
15. Katsuki, D.; Ohmura, R.; Ebinuma, T.; Narita, H. Formation, growth and ageing of clathrate hydrate crystals in a porous medium. *Phil. Mag.* **2006**, *86*, 1753–1761.
16. Katsuki, D.; Ohmura, R.; Ebinuma, T.; Narita, H. Methane hydrate crystal growth in a porous medium filled with methane-saturated liquid water. *Phil. Mag.* **2007**, *87*, 1057–1069.
17. Katsuki, D.; Ohmura, R.; Ebinuma, T.; Narita, H. Visual observation of dissociation of methane hydrate crystals in a glass micro model: Production and transfer of methane. *J. Appl. Phys.* **2008**, *104*, 083514:1–083514:9.
18. Yoon, Y.S.; Lee, S.H.; Seong, K. Convective heat transfer coefficient at hydrate pellet surface during regasification. In *Proceedings of the 7th International Conference on Gas Hydrates*, Edinburgh, Scotland, UK, 17–21 July 2011.
19. Tanaka, S. Heat Transfer Analysis of Re-gasification of Packed Bed of Hydrates. In *Proceedings of the 7th International Conference on Gas Hydrates*, Edinburgh, UK, 17–21 July 2011.
20. Liu, B.; Pang, W.; Peng, B.Z.; Sun, C.Y.; Chen, G.J. Heat transfer related to gas hydrate formation/dissociation. *Developments in Heat Transfer*; InTech: Rijeka, Croatia, 2010; pp. 477–502.
21. Pang, W.X.; Xu, W.Y.; Sun, C.Y.; Zhang, C.L.; Chen, G.J. Methane hydrate dissociation experiment in a middle-sized quiescent reactor using thermal method. *Fuel* **2009**, *88*, 497–503.

22. Zhang, X.; Lu, X.; Li, Q.; Yao, H. Thermally induced evolution of phase transformations in gas hydrate sediment. *Sci. China Phys. Mech. Astron.* **2010**, *53*, 1530–1535.
23. Kamth, V.A. Study of heat transfer characteristics during dissociation of gas hydrates in porous media. Ph.D. Thesis, University of Pittsburgh, Pittsburgh, PA, USA, January 1984.
24. Sloan, E.D. *Clathrate Hydrates of Natural Gases*; CRC Press: Boca Raton, FL, USA, 2008; pp. 609–615.
25. Makogon, Y.F. *Hydrates of Natural Gas*; Penn Well Publishing Company: Tulsa, OK, USA, 1987.
26. Su, K.; Sun, C.; Yang, X.; Chen, G.; Fan, S. Experimental investigation of methane hydrate decomposition by depressurizing in porous media with 3-Dimension device. *J. Nat. Gas Chem.* **2010**, *19*, 210–216.
27. Makogon, Y.F. *Hydrates of Hydrocarbons*; PennWell Publishing Company: Tulsa, OK, USA, 1997; pp. 245–248.
28. Wang, X. *Engineering of Heat and Mass Transfer (in Chinese)*; Science Press: Beijing, China, 1998; Volume 2, pp. 322–342.

© 2012 by the authors; licensee MDPI, Basel, Switzerland. This article is an open access article distributed under the terms and conditions of the Creative Commons Attribution license (<http://creativecommons.org/licenses/by/3.0/>).